Effects of Coulomb distortion and final state interaction on the fourth and fifth structure functions

Yanhe Jin, D. S. Onley, and L. E. Wright
Institute of Nuclear and Particle Physics, Department of Physics and Astronomy, Ohio University, Athens, Ohio 45701
(Received 30 December 1993)

We examine the question of whether the fourth and fifth structure functions (called W_{LT} and $W_{LT'}$) defined by the plane wave Born approximation (PWBA) for the reaction $(e,e'p)$ are still meaningful quantities in the presence of electron Coulomb distortion. For a heavy target (^{208}Pb), the apparent structure functions obtained in the presence of the electron Coulomb distortion have shapes (in terms of the number of maxima or minima) similar to those defined in PWBA; however, the magnitudes are changed greatly. For the fourth structure function, the distortion can change the magnitude, even for ^{16}O, by more than 15%. For proton knockout from $(l \pm \frac{1}{2})$ spin-orbit doublet states, the changes caused by electron distortion have opposite effects, increasing the magnitude of the one while decreasing the other. The Coulomb effects on the fifth structure function depend on the out of plane angle used in the extraction. For a small angle (e.g., 10°), the electron distortion can be more than 15% in ^{16}O. However, for certain kinematic choices, the Coulomb distortion effects on the fifth structure function can largely be removed. For proton knockout from spin-orbit doublet states the ratio of the fifth structure functions is of interest. We find that this ratio is nearly independent of the central part of the proton final state interaction and has the power of investigating the spin-orbit interaction of optical potentials.

PACS number(s): 25.30.Bf

I. INTRODUCTION

Electron scattering in the quasielastic region provides an excellent tool for studying nuclear structure and understanding the dynamics of the nucleon response in nuclei as a function of the energy and momentum transfer. In the plane wave Born approximation (PWBA), in which the electrons are represented by plane waves, the cross section can be written in terms of structure functions, which in turn can be related to bilinear combinations of the four-current components in momentum space. Various authors [1,2] have given detailed formulas for the decomposition of the PWBA cross section into products of electron kinematic factors and structure functions using the fact that the potential generated by the plane wave electrons can be separated into so-called longitudinal and transverse parts with respect to the momentum transfer direction. Unfortunately, these two references use somewhat different notation and definitions (involving factors of the square root of 2) for the electron kinematic factors which lead to corresponding differences in the structure functions. We give our conventions below, which follow those of Donnelly [1].

Since the structure functions appear in the cross section with different electron kinematic factors, one can, in principle, study them independently. However, when one tries to separate these structure functions, two precautions have to be kept in mind. The first is whether or not the PWBA formalism is valid, since, in the presence of Coulomb distortion, the structure functions no longer appear in the formalism. We will discuss this point further when we discuss the $(e,e'p)$ reaction. The second is, even if the PWBA is valid, do the measured cross section data contain enough information to allow one to separate out a particular structure function? We have discussed elsewhere [3] the difficulties of separation of the longitudinal and transverse structure functions in quasielastic (e,e') reactions.

Since coincidence experiments select a particular reaction channel to be measured, exclusive $(e,e'p)$ experiments in the quasielastic region furnish a very clean tool for studying single-particle properties of the nucleus, and have provided a testing ground for different nuclear models [4,5]. High-resolution experiments have been carried out on a range of nuclei at NIKHEF-K [5–9] in Amsterdam and at Saclay [10]. Relativistic Hartree bound state orbitals or other reasonable nonrelativistic wave functions, coupled with appropriate optical potentials for the continuum proton, furnish a good description of these experimental data and permit the extraction of spectroscopic factors [11–14]. However, different optical potentials, although they fit the elastic scattering observables, can lead to different spectroscopic factors [12]. Thus the current analyses do not provide completely unique spectroscopic factors and do not discriminate one optical potential from another. However, the fourth and fifth structure functions (corresponding to two different longitudinal-transverse interference terms) might be used to provide some discriminatory power especially as the fifth structure function is known to vanish in the absence of proton final state interactions [15]. Extraction of the fifth structure function does require a polarized electron beam.

However, as we mentioned as our first precaution, electron Coulomb distortion destroys the precise relationship of these structure functions to the cross section.

In this paper, we examine the consequences of following the PWBA prescription for separating the structure functions in the presence of electron Coulomb distortion. Are the apparent structure functions so obtained still meaningful quantities? In particular, we are interested in examining the fourth and the fifth structure functions, which embody left-right and up-down asymmetries of the cross section measured with respect to the momentum transfer direction ($\vec{q}$).

In Sec. II we briefly introduce the theoretical model used for the calculation and compare the PWBA formalism for $(e,e'p)$ with a distorted wave Born approximation (DWBA) formalism for $(e,e'p)$; we introduce the distinction between the structure functions and the apparent structure functions. In Sec. III, we consider Coulomb effects on the fourth structure function and consider similarly, in Sec. IV, the fifth structure function. In Sec. V, we discuss how to use these left-right and up-down asymmetries of the nuclear response to study the final state interaction, namely the optical potentials used for the knocked-out proton. And finally we will give our conclusion in Sec. VI. Throughout we use ^{16}O, ^{40}Ca and ^{208}Pb as sample target nuclei.

II. THEORETICAL MODEL

We choose to work in the laboratory frame of reference in which the target nucleus is at the origin of the coordinate system. The incoming electron with four-momentum $k^\mu = (k_0, \vec{k})$ and the scattered electron with $k'^\mu = (k'_0, \vec{k}')$ define the scattering plane (x-z plane). The knocked-out proton with $p^\mu = (E, \vec{p})$ [described by the polar angles (θ_p, ϕ_p)] and the four-momentum transfer $q^\mu = k^\mu - k'^\mu = (\omega, \vec{q})$ define the reaction plane. Following the PWBA convention, we choose $\hat{\mathbf{z}}$ along the q direction and in this case the angle between the scattering plane and the reaction plane is just ϕ_p. Throughout we use units such that $(\hbar = c = 1)$.

In the plane wave Born approximation (PWBA), the cross section for $(\vec{e}, e'p)$ can be written as

$$\frac{d^3\sigma}{dk'd\Omega_e d\Omega_p} = K(v_L W_L + v_T W_T + v_{TT} W_{TT}\cos 2\phi_p + v_{LT} W_{LT}\cos\phi_p + h v_{LT'} W_{LT'}\sin\phi_p) \quad (1)$$

where h is the incident electron helicity, $K = Ep\sigma_{\rm Mott}/(2\pi)^3$, and the factors v_L, v_T, etc, depend only on electron kinematics. In this paper we are only concerned with the so-called fourth and fifth structure functions W_{LT} and $W_{LT'}$. The electron kinematic factors for these are given by

$$v_{LT} = \frac{1}{\sqrt{2}}\left(\frac{-q_\mu^2}{\vec{q}^2}\right)\left(\frac{-q_\mu^2}{\vec{q}^2} + \tan^2\frac{\theta}{2}\right)^{\frac{1}{2}}, \quad (2)$$

$$v_{LT'} = \frac{1}{\sqrt{2}}\left(\frac{-q_\mu^2}{\vec{q}^2}\right)\tan\frac{\theta}{2}. \quad (3)$$

The fourth structure function can be written as

$$W_{LT} = -\sqrt{2}\mathrm{Re}[J_0^* J_x], \quad (4)$$

where $J^\mu = (J_0, \vec{J})$ is the Fourier transform of the transition current. Thus W_{LT} is the interference between the transition charge J_0 and the transverse component of the transition current in the scattering plane J_x. The fifth structure function is defined by

$$W_{LT'} = -\sqrt{2}\mathrm{Re}[J_0^* J_y] \quad (5)$$

which looks like the fourth structure function except the component of the transition current involved is in the direction perpendicular to the scattering plane. The definitions of the other kinematic factors and structure functions are given in Ref. [1].

From Eq. (1) we can see that the fourth structure function W_{LT} could be obtained experimentally by subtracting the cross sections with $\phi_p = 0$ and $\phi_p = \pi$ while keeping other electron and proton kinematic variables the same. We will call a quantity so determined the *apparent* structure function. This amounts to looking at protons coming out in the (e,e') scattering plane and determining left-right asymmetry with respect to the momentum transfer direction. Thus

$$W_{LT}^d = \frac{\sigma^R - \sigma^L}{2Kv_{LT}}, \quad (6)$$

where L (left) indicates the $\phi_p = 0$ case and R (right) indicates $\phi_p = \pi$. The superscript d is to indicate that the apparent structure function W_{LT}^d includes electron Coulomb distortion. If one can ignore the electron Coulomb distortion, then $W_{LT}^d = W_{LT}$, the plane wave result. Similarly, if the incident electron beam is polarized (say, h=1), one can compare the cross section for $0 < \phi_p < \pi$ [above the plane or "up" (U)] and the cross section at $-\phi_p$ [below the plane or "down" (D)] while keeping all other kinematical variables the same. The apparent fifth structure function is then

$$W_{LT'}^d = \frac{\sigma^U - \sigma^D}{2Kv_{LT'}\sin\phi_p}, \quad (7)$$

which reflects the up-down asymmetry of the measured cross section with respect to the scattering plane, and clearly requires out of plane measurements.

In case one includes electron Coulomb distortion, the actual fourth and fifth structure functions are still defined by Eqs. (4) and (5), but one can determine from experiment, or a DWBA calculation, only the left-right asymmetry and up-down asymmetry given in Eqs. (6) and (7) and hence the apparent structure functions. For a given nuclear model the expressions of Eqs. (4) and (5) and Eqs. (6) and (7) can be calculated and their differences reflect the effect of the electron Coulomb distortion, which is one of the primary subjects of this paper.

In distorted wave Born approximation (DWBA) calculations, we use Coulomb distorted waves for the electrons, and the differential cross section takes on a different form from Eq. (1):

$$\frac{d^3\sigma}{dk'd\Omega_e d\Omega_p} = 2\pi\rho_e\rho_p\sum|H_i|^2, \quad (8)$$

where the summation is over the final states with an average over the initial states, ρ_e, ρ_p are the density of states for electron and proton, respectively, and H_i is the transition matrix element,

$$H_i = -4\pi \int j_\mu(r) G(r,r') J^\mu(r') d^3r d^3r'. \quad (9)$$

This matrix element is composed of the electron current

$$j_\mu = \bar{\psi}_f \gamma_\mu \psi_i \quad (10)$$

evaluated using distorted waves ψ_i and ψ_f which are solutions to the Dirac equation with the static Coulomb potential of the target nucleus included and are given in terms of partial wave expansions. The nuclear current J^μ is also expressed as a partial wave decomposition. Here the current is understood to be in configuration space rather than momentum space as in Eqs. (4) and (5) but is otherwise the same quantity. The Green's function for the electromagnetic field is denoted by $G(r,r')$. To proceed further we must adopt a specific model for J^μ. We take the free nucleon current operator and write

$$J^\mu = \langle \bar{\Psi}_f | F_1 \gamma^\mu + F_2 \frac{i\mu_p}{2M} \sigma^{\mu\nu} q_\nu | \Psi_i \rangle, \quad (11)$$

where F_1 and F_2 are the Dirac and Pauli nucleon form factors. The detailed description of the conventions and notation is given in Ref. [11]. The wave function we use for the bound state Ψ_i is from a relativistic Hartree model. The final state wave function Ψ_f we use is obtained by solving the Dirac equation with an optical potential which comes from the analysis of elastic proton scattering data. We can also use nonrelativistic optical potential models through the relativistic UT transformation [16].

One should notice that the apparent fourth and fifth structure functions [Eqs. (6), (7)] may be expected to depend on the specifics of the electron kinematics as compared with the *actual* structure functions [Eqs. (2), (3)], which depend on energy and momentum transfer only. This point is important because when one tries to compare a DWBA calculation with the experimental data, one should use the same electron kinematics as used in the experiment.

III. THE LEFT-RIGHT ASYMMETRY OF THE NUCLEAR RESPONSE

The apparent fourth structure function W^d_{LT} defined in Eq. (6) is a measure of the left-right asymmetry of the nuclear response with respect to the $\vec{q}$ direction. Another measure might be just the ratio of the left and right reduced cross sections; we will discuss the advantage of this choice at the end of this section.

To look at Coulomb distortion effects on the fourth structure function, we choose three cases in which the protons are knocked out from the outer orbitals of ^{16}O, ^{40}Ca, and ^{208}Pb. Initially we examine the $p_{1/2}$, $d_{3/2}$, and $3s_{1/2}$, orbitals, respectively. The incident electron energy is 500 MeV, the proton kinetic energy is $T_p = 100$ MeV, and we choose kinematics such that the outgoing proton momentum p is equal to the momentum transfer q.

It has been suggested [4] that the electron Coulomb distortion effect is of the order of 3% for ^{16}O, 7% for ^{40}Ca, and 30% for ^{208}Pb. These estimates may be realistic for the cross sections, but the fourth structure function involves the subtraction of two values of the cross section which are not too different in size. The Coulomb distortion correction may be different, possibly even having the opposite sign for the two points in question, and can be a significant part of the difference. To examine this point, the apparent fourth structure functions for the three cases considered are shown in Fig. 1, and we can see that indeed the effect of Coulomb distortion on the fourth structure function does not obey this simple estimate. For ^{16}O, Coulomb distortion can change the plane wave result by more than 15%, and by more than a factor of 2 for ^{208}Pb. From these calculations we learn two things: (1) Coulomb distortion has a much larger effect on the fourth structure function than on the cor-

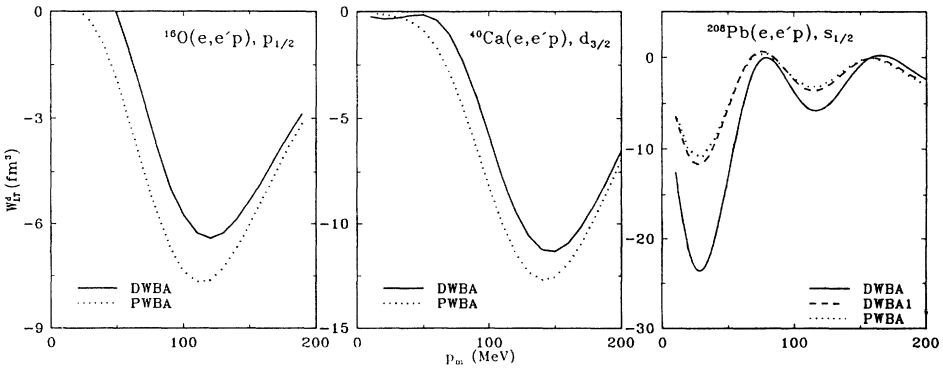

FIG. 1. The apparent fourth structure function R_{LT} for outer orbitals from ^{16}O,^{40}Ca, and ^{208}Pb as a function of missing momentum p_m. The electron incident energy is 500 MeV. Proton kinetic energy is 100 MeV. The momentum transfer $q = p$ where p is the outgoing proton momentum. The solid lines are DWBA calculations and the dotted lines are PWBA calculations. The dashed line for the ^{208}Pb case is the DWBA calculation with $Z = 1$.

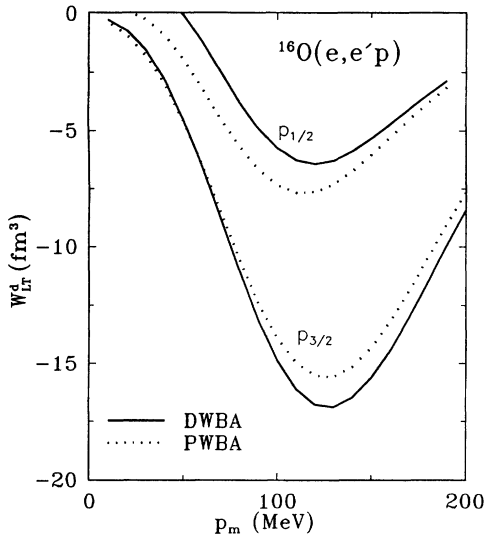

FIG. 2. The apparent fourth structure function compared for a proton knockout from spin-orbit doublet states $p_{1/2}$, $p_{3/2}$ of ^{16}O. Kinematics are the same as in Fig. 1.

responding cross section and the sign of the correction is sometimes positive and sometimes negative (see below); (2) the basic shape generated by the DWBA calculation is roughly the same as the PWBA calculation in terms of number of maxima and minima. It appears that these shapes are mainly determined by the physics involved; i.e., on which parts of the transition current and transition density are involved. Thus with the use of suitable scale factors it might be possible to reconstruct the true structure function from the apparent one.

We also did a $p_{3/2}$ proton knockout calculation for ^{16}O, and together with the $p_{1/2}$ calculation we show the results in Fig. 2. We can see that the electron Coulomb distortion has a different effect on each of the $l \pm \frac{1}{2}$ spin-orbit doublet states. It increases the magnitude of the $l + \frac{1}{2}$ proton knockout but decreases that of the $l - \frac{1}{2}$ proton knockout. This explains the different effects for $p_{1/2}$ and $d_{3/2}$ orbitals as compared to the $s_{1/2}$ orbital in Fig. 1.

Fourth structure function separation extractions for ^{16}O have been published by the Saclay group [10]. We intend to make a detailed analysis of this experiment and recently reported ^{16}O data from NIKHEF [5] at a later time. In Figs. 3 and 4 we show our DWBA and PWBA calculations for the kinematics of the Saclay experiment. A best fit of the DWBA cross section (Fig. 3) for the two orbitals leads to spectroscopic factors of 0.54 (for $p_{1/2}$) and 0.57 (for $p_{3/2}$). These are to be compared with 0.64 and 0.71 obtained in the original analysis. In our calculation we just used bound state orbitals from a relativistic Hartree calculation and made no attempt to adjust the effective single-particle wave function to fit the cross section, other than to scale the overall result by a spectroscopic factor. In Fig. 4 we show the apparent (DWBA) and true (PWBA) structure functions extracted from the cross section as compared to the values extracted from the experimental measurement in Ref. [10]. The calculated curves are scaled by the spectroscopic factors of 0.54 and 0.57, respectively. One of the conclusions of Ref. [10] was that theoretical calculations for the fourth structure function and for the cross section need different scale factors (spectroscopic factors) in order to bring both into agreement with data. On the other hand, we find reasonable agreement between our calculation and the extracted structure function; however, based on the data provided in Ref. [10], we believe that the extracted W_{LT} may not be too well determined and note that the error bars shown (in Fig. 4) are from our own estimate. In addition, Coulomb distortion affects this conclusion significantly since it is evident that the Coulomb effect on the peaks of the cross section is of order 3–4% while it is of order 12–15% for the structure functions.

As noted in Ref. [10], another quantity that can be used to represent the left-right asymmetry is the ratio

$$R_{LR} = \frac{\rho(\vec{p}_m)^L}{\rho(\vec{p}_m)^R}. \tag{12}$$

The reduced cross section $\rho(\vec{p}_m)$ is the five-fold differ-

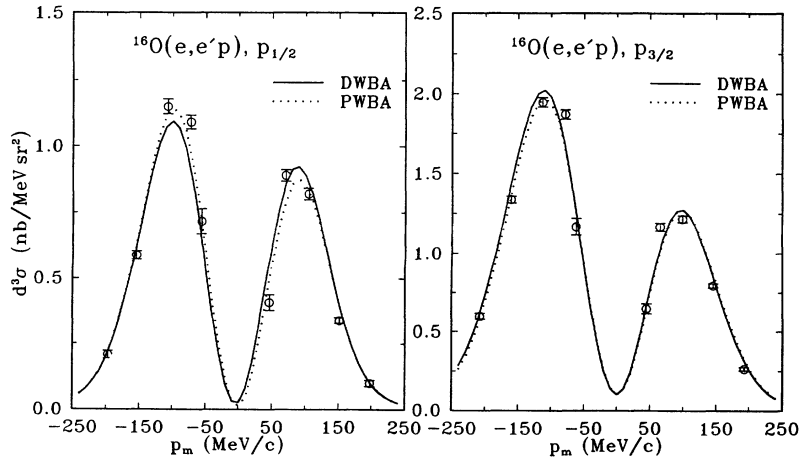

FIG. 3. The DWBA and PWBA calculations of the cross section for the two p states compared with the experimental data [10]. The curves are scaled by 0.54 for $p_{1/2}$ and 0.57 for $p_{3/2}$.

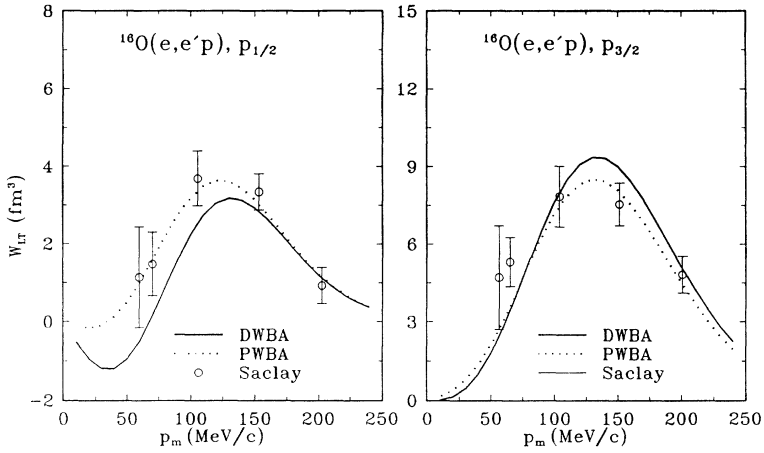

FIG. 4. The apparent fourth structure function (DWBA) and the actual fourth structure function (PWBA) for the two p states is compared to the experimentally extracted values [10]. The curves are scaled by 0.54 for $p_{1/2}$ and 0.57 for $p_{3/2}$. Note that the data points of Ref. [10] have been multiplied by 0.707 to match our convention for W_{LT}.

ential cross section divided by the electron-proton cross section σ_{ep}^{cc1} [17]; this quantity is traditionally written in terms of the missing momentum $\vec{p}_m = \vec{p} - \vec{q}$. In taking the ratio of the reduced cross section on the left of $\vec{q}$ with that on the right of $\vec{q}$ much information about the target nucleus gets canceled out, including the spectroscopic factor. However, the electron Coulomb distortion and the proton final state interaction do effect R_{LR}. Without electron Coulomb distortion and proton final state interaction we have $R_{LR} \approx 1$. The ratio R_{LR} uses the same aspects of the cross section as the fourth structure function, but has the advantage that it depends little on the nuclear structure but is sensitive to the final state interaction. We suggest it might be used to investigate the effect of different optical potentials.

In Fig. 5, we show calculations of this ratio for the two outermost orbitals of ^{16}O. We should mention that Fig. 2 and Fig. 5 result from the same cross section calculations, but they single out different information from the cross sections. The dotted lines are PWBA calculations

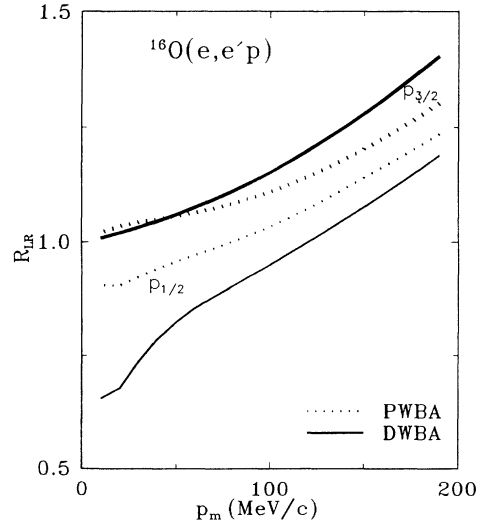

FIG. 5. The same calculation as Fig. 2, but the asymmetry is represented by the ratio of the reduced cross sections measured at the left and right sides of the $\hat{\mathbf{q}}$ direction.

(electron plane waves) where the final state interaction of the knocked-out proton is retained. The solid lines are DWBA calculations. The difference between the dotted and solid lines represents the effect of the electron distortion. While there is no experimental way to separate the electron Coulomb distortion from the proton final state interaction, we can use the fact that the interaction of the electron is well known and can be calculated to any required accuracy knowing only electron elastic scattering. Hence the electron distortion can always be accounted for, and in this sense we can say the only unknown contribution to R_{LR} is from the proton final state interaction.

IV. THE UP-DOWN ASYMMETRY OF THE NUCLEAR RESPONSE

Using a polarized electron beam and detecting protons ejected out of the (e, e') scattering plane allows the extraction of the fifth structure function $W_{LT'}$ which is a measure of the up-down asymmetry of the nuclear response. In PWBA, the fifth structure function has a nonzero value only when one includes the final state interaction [15]. It is hoped that measurement of this quantity can provide additional information on the optical potential as well as nuclear structure. However, as mentioned in the Introduction, one has to make sure the electron distortion effect does not destroy the PWBA picture. We again choose three cases in which the protons are knocked out from the outermost states for ^{16}O, ^{40}Ca, and ^{208}Pb, i.e., from $p_{1/2}$, $d_{3/2}$, and $3s_{1/2}$, respectively. The incident electron energy is again 500 MeV, the proton kinetic energy is $T_p = 100$ MeV, and p equals q.

We first look at Coulomb distortion effects on the measurement of the fifth structure function for the case of ^{16}O. In PWBA, the fifth structure function does not depend on the angle ϕ_p; however, electron distortion destroys this independence. In Fig. 6, we show the DWBA calculations of the apparent fifth structure function at two ϕ_p angles (20°,40°). The solid lines represent the distorted wave calculations or apparent structure function and the dotted line represents the plane wave calcu-

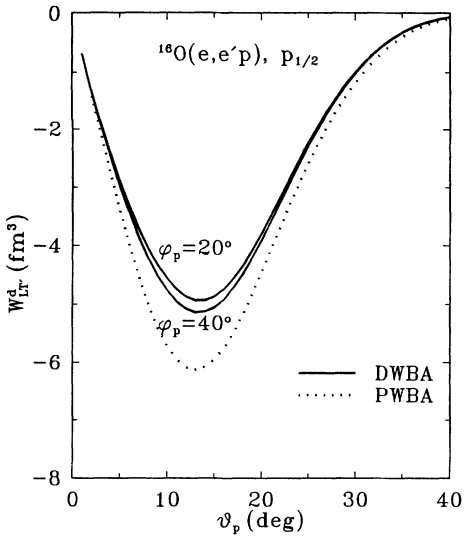

FIG. 6. The apparent fifth structure function $W_{LT'}$ for quasielastic scattering from the $d_{3/2}$,$d_{5/2}$ states of ^{40}Ca. The Coulomb effect has destroyed the ϕ_p independence of the PWBA description. The DWBA calculations are done using two out of scattering plane angles, $\phi_p = 20°,40°$.

lation or actual structure function. We can see that (1) the Coulomb effect is more than 12%, and (2) there is a clear ϕ_p dependence in the DWBA calculations. Since the dependence seems to be mainly a magnitude change, we calculated the DWBA fifth structure function at the peak value ($\theta_p = 14°$) as a function of ϕ_p which is shown by the solid line in Fig. 7. We see that at $\phi_p = 90°$ the apparent and true structure functions become equal. Furthermore, if we average the apparent structure function over ϕ_p it agrees with the actual structure function to within 1%. Of course, Coulomb distortion for ^{16}O is not so great, so we repeated these calculations for the same case except we changed the charge seen by the electrons from $Z = 8$ to $Z = 20$. This result is the dashed line in Fig. 7. While the crossing of the apparent and actual structure functions moved forward from $\phi_p = 90°$ somewhat and the average of the apparent structure functions exceeds the actual structure function by about 5%, it does appear that measurement at $\phi_p = 90°$ or averaging over ϕ_p largely removes Coulomb distortion effects from the measured fifth structure function.

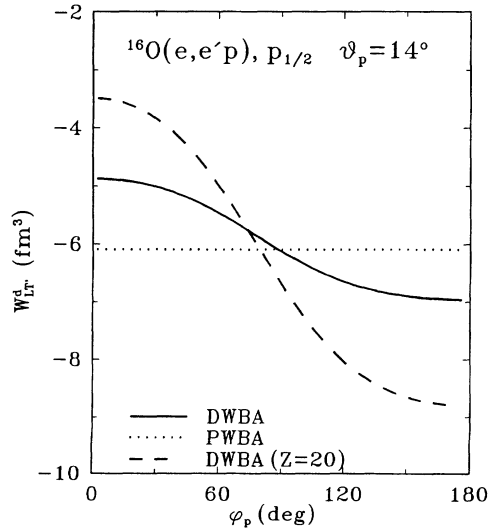

FIG. 7. The apparent fifth structure function as a function of reaction-plane angle ϕ_p for the $p_{1/2}$ state of ^{16}O. The proton polar angle $\theta_p = 14°$. The dashed line is the same result but with Z=20.

In Fig. 8, we show DWBA calculations of the fifth structure function for ^{40}Ca and ^{208}Pb at fixed reaction-plane angle $\phi_p = 40°$. These curves show the effect of increasing the electron Coulomb distortion on the measurement of the fifth structure function. Again, as we learned from the fourth structure function, the electron Coulomb distortion does not change the basic shape of the fifth structure function although the amplitudes are changed considerably.

One could also use the ratio of the measured cross sections at up ($0 < \phi_p < \pi$) and down ($-\phi_p$) directions to study the up-down asymmetry of the reduced cross section, namely,

$$R_{UD} = \frac{\rho(\vec{p}_m)^U}{\rho(\vec{p}_m)^D}. \tag{13}$$

Again, the advantage of this quantity is that it can be compared directly to single-particle model calculations since it does not require any spectroscopic factor. It might provide additional information for studying optical potential models.

V. OPTICAL POTENTIALS AND UP-DOWN, LEFT-RIGHT ASYMMETRY

The $(e,e'p)$ process in the quasielastic region provides a tool for studying optical potentials. It is known that the optical potential obtained from elastic proton scattering coupled with a single-particle shell model provide a fairly good description of the current $(e,e'p)$ experimental cross section data. However, different optical potentials determined from elastic proton scattering can differ in the interior of the nucleus since only the phase shifts are used in calculating scattering observables. The interior part of the wave function is needed in reaction cross sections, particularly in the $(e,e'p)$ process. If one could find experimental observables which distinguish different final state interactions while being relatively insensitive to details of the primary reaction, one could obtain much useful information. The left-right asymmetry ratio R_{LR} and up-down asymmetry ratio R_{UD} provide such quantities because they depend on the proton final state interaction only. In the following, we will also demonstrate that the final state spin-orbit interaction might be characterized by the ratio of the fifth structure functions obtained for protons from spin-orbit doublet states ($j = l \pm 1/2$) of the target nucleus. In this section, we will concentrate

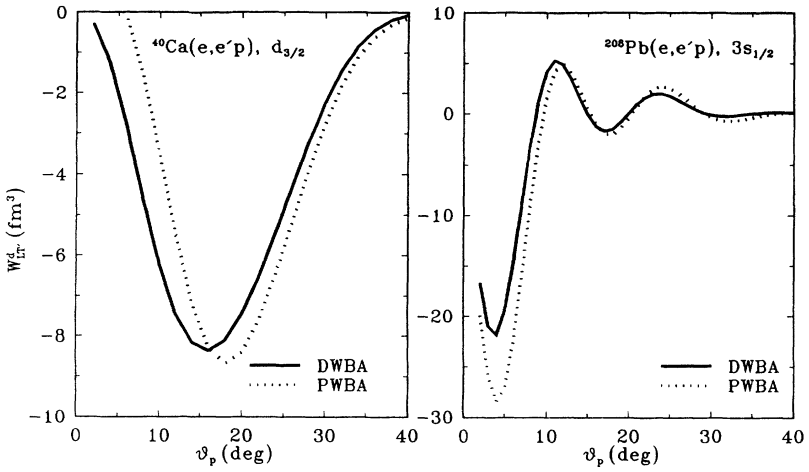

FIG. 8. $W^d_{LT'}$ for ^{40}Ca and ^{208}Pb targets. The reaction-plane angle is $\phi_p = 40°$.

on the proton final state interaction and use PWBA for all calculations unless otherwise specified. It should be understood that, when one wants to compare the calculations with experimental data, electron Coulomb distortions should be included.

For the different optical models we will use a relativistic global optical potential [18,19], its UT [16] form which is a phase-equivalent relativistic potential with some nonrelativistic characteristics, and a nonrelativistic global optical potential developed by Schwandt and coworkers [20]. These potentials are available for ^{40}Ca which we choose as our target in the following calculations. The two global potentials are widely used in the analysis of the $(e, e'p)$ experimental data, and the UT form is introduced as it has characteristics intermediate between the conventional relativistic and nonrelativistic potentials.

We first look at the sensitivity of the left-right asymmetry measurement R_{LR} to the different optical potentials. In Fig. 9, the solid line is the calculation, using the relativistic global optical potential, the dashed line is a UT model calculation, and the dotted line is a calculation using the Schwandt potential. The peak of the calculated cross section is around $p_m = 120$ MeV/c. The difference between the dashed line and the solid line shows the effect of using a relativistic optical potential. We can see that this effect is about 4% around the peak (of the cross section), which would require a high precision experiment to tell the difference. The difference between the dotted line and dashed line is very small, which means the quantity R_{LR} cannot distinguish between a relativistic UT optical potential and the nonrelativistic potential. However, as we will show in the following, some observables can tell the difference between these two potentials.

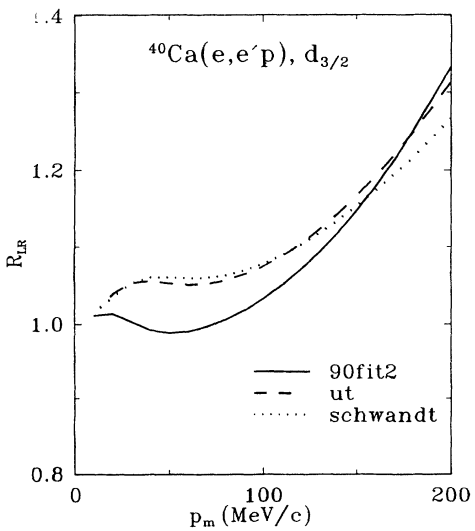

FIG. 9. Calculations of R_{LR} using different optical potential models. The curve labeled 90fit2 is a relativistic global model [18]; the UT model is phase-shift equivalent to 90fit2, but with a nonrelativistic character [16]; the Schwandt potential is nonrelativistic [20].

We next investigate the fifth structure function for studying different optical potentials. Although it is well known that $W_{LT'}$ is entirely due to the final state interaction of the knocked-out nucleon with the residual nucleus [15], it remains to be seen how this function can be used to distinguish the contributions of different components in the final state interaction.

Since most of the information about the nuclear structure is contained in the bound state density or momentum distribution, in order to study the final state interaction, one can largely separate out the contribution of the bound state by using spin-orbit doublet states $l \pm \frac{1}{2}$, since the densities would be approximately the same for $l + \frac{1}{2}$ and $l - \frac{1}{2}$ states. This suggests that we use the ratio

$$R^W_{LT'} = W_{LT'}(l + \tfrac{1}{2})/W_{LT'}(l - \tfrac{1}{2}). \tag{14}$$

In the following, we demonstrate how this quantity depends on the final state interaction. Notice that in this comparison we have set both spectroscopic factors equal, although this would normally not be the case. The factors would be obtainable directly from comparison of the measured cross sections and the calculations.

In Fig. 10 we show the results of knocking out a proton from both the $d_{3/2}$ state (shown by thick curves) and the $d_{5/2}$ state (thin curves). The optical potential used is that of Schwandt. The proton energy is 100 MeV and we have set $p = q$. We want to examine how the fifth structure function depends on the different parts of the

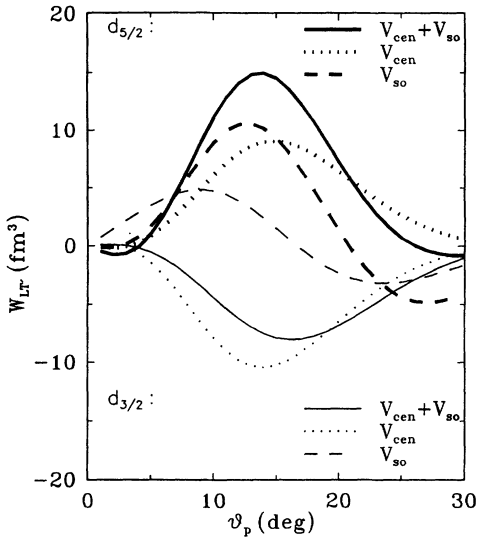

FIG. 10. Calculations for knocking out a $d_{5/2}$ proton (thick curves) and a $d_{3/2}$ proton (thin curves). The target nucleus is ^{40}Ca. The dotted lines result from using only the central potential, the dashed lines from using only the spin-orbit potential, and the solid lines result from using the full optical potential.

optical potential. First, the spin-orbit potential is set to zero. $W_{LT'}$ still takes on a large value when calculated for the two spin-orbit doublet states, and although it has a different sign, the magnitudes around the peak are about the same. This means that if we take the ratio, the value is about -1 at the peak, which is shown by the dotted line in Fig. 11. The fact that this ratio is very close to -1 in a large range around the peak suggests that the ratio $R^W_{LT'}$ is nearly independent of the final state central potential. Next we examine the spin-orbit interaction by turning off the central potential; we see by the dashed lines in Fig. 10 that the spin-orbit potential increases the magnitudes of $W_{LT'}$ by different amounts for the $d_{3/2}$ and $d_{5/2}$ cases. The solid lines are the calculations using the full potential. As can be seen, the combined central and spin-orbit results for $d_{3/2}$ and $d_{5/2}$ are very different, which means the ratio $R^W_{LT'}$ will have a value quite different from -1, and the difference will depend on the final state spin-orbit interaction. It appears that $R^W_{LT'}$ should be a good measure of the final state spin-orbit interaction. We have calculated this ratio using various optical potentials. In Fig. 11 we show three calculations: the solid line uses the relativistic optical potential, the dotted line uses the Schwandt nonrelativistic potential, and the dashed line is the UT calculation. Evidently, around the angle $\theta_p = 15°$, which is the peak of $W_{LT'}$, one can distinguish one optical potential from the others.

Another aspect we have investigated is the dependence of $R^W_{LT'}$ on the momentum transfer q. Because the q dependence of the current J_μ is determined by the r dependence of the corresponding wave functions, we expect that the q dependence of $R^W_{LT'}$ can provide some information about the r dependence of the optical potential. In quasielastic experiments, if one keeps the proton scattering angle θ_p and the proton kinetic energy fixed, one can still vary q (p_m will change) in measuring the cross section. In Fig. 12, we show calculations corresponding to such kinematics with a proton kinetic energy of 100 MeV. The proton angle is fixed at 15°, which is roughly at the peak of the $W_{LT'}$ over the q range chosen. We see that the differences caused by using different optical potentials depend on the value of q very sensitively: as one goes to higher q values, the differences can be quite large (as much as a factor of 2 as shown here).

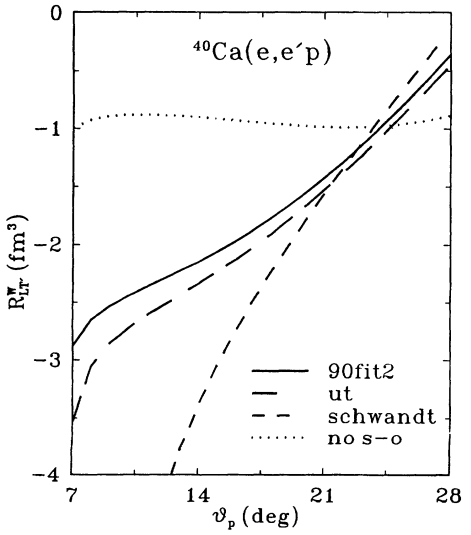

FIG. 11. Calculations of $R^W_{LT'}$ as a function of θ_p using different optical potentials. The dotted line (no s-o) omits the spin-orbit part from the Schwandt potential.

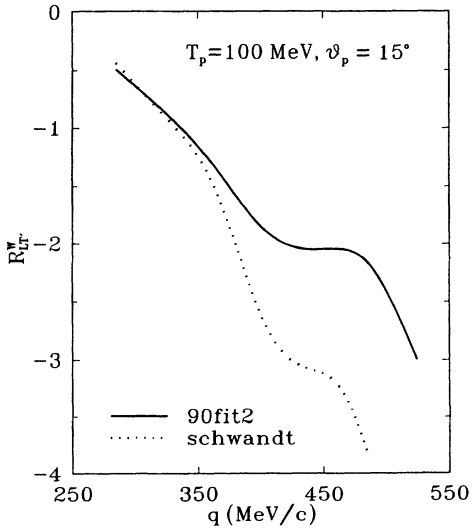

FIG. 12. Calculations of $R^W_{LT'}$ as a function of q using different optical potentials.

VI. CONCLUSION

The apparent fourth and fifth structure functions extracted from experiments can provide additional insight into nuclear structure and final state interactions. Even though the procedure prescribed by the plane wave Born approximation no longer gives rise to a well defined function of nuclear current in the presence of electron Coulomb distortion, one can still usefully extract apparent fourth and fifth structure functions from the experimental data using the PWBA formalism. The Coulomb distortion of these two structure functions does not change the shape appreciably. Even for a target as heavy as ^{208}Pb, the apparent fourth and fifth structure functions still have the same shapes (in terms of the number of maxima or minima) as the ones given by the PWBA; however, the magnitudes are greatly affected by Coulomb distortion. These changes are much greater than the corresponding changes to the cross section. Even for ^{16}O, the magnitude change due to electron Coulomb distortion in the fourth structure function is more than 15% at the Saclay kinematics. The change in the magnitude of the fifth structure function depends on the out of plane angle ϕ_p used in the extraction procedure. Extraction of the fifth structure function around $\phi_p = 90°$, or averaging the fifth structure function over ϕ_p, greatly reduces the Coulomb effect.

Different optical potentials, which describe the same elastic proton scattering observables, can be very different in the interior. While the $(e, e'p)$ cross section analyses have some slight shape dependence on the optical potential used, the primary effect is on the magnitude and hence on the value of the spectroscopic factors extracted. In this paper, we have shown that examination of subsets of the $(e, e'p)$ cross section data can provide additional discriminatory power. In particular, we have shown that R_{LR}, the ratio of reduced cross sections on the left as compared to the right of the momentum transfer direction, is sensitive to the optical potential. The fifth structure function is also sensitive to the optical potential and the ratio of fifth structure functions $R^W_{LT'}$ for spin-orbit doublets is very sensitive to the spin-orbit term in the optical potential. In principle, the quantity R_{LR} can provide insight as to whether one should use relativistic or nonrelativistic wave functions, but one needs high precision experiments.

ACKNOWLEDGMENTS

We would like to thank the Ohio Supercomputer Center for providing the Cray Y-MP time to carry out the necessary calculations. This work was supported in part by the U.S. Department of Energy under Grant No. DE-FG02-87ER40370.

[1] T.W. Donnelly, in *Perspectives of Nuclear Physics at Intermediate Energies*, edited by S. Boffi, C. Ciofi degli Atti, and M.M. Giannini (World Scientific, Singapore, 1983), p. 305.
[2] A. Picklesimer and J.W. Van Orden, Phys. Rev. C **40**, 290 (1989).
[3] Yanhe Jin, D.S. Onley, and L.E. Wright, Phys. Rev. C **45**, 1333 (1992).
[4] S. Frullani and J. Mougey, Adv. Nucl. Phys. **14**, 1 (1984).
[5] L. Lapikás, Nucl. Phys. **A553**, 297c (1993).
[6] G. van der Steenhoven, H.P. Blok, E. Jans, L. Lapikás, E.N.M. Quint, and P.K.A. de Witt Huberts, Nucl. Phys. **A484**, 445 (1988).
[7] J.W.A. den Herder, H.P. Blok, E. Jans, P.H.M. Keizer, L. Lapikás, E.M.N. Quint, G. van der Steenhoven, and P.K.A de Witt Huberts, Nucl. Phys. **A490**, 507 (1988).
[8] E.M.N. Quint, Ph.D. dissertation, University of Amsterdam, 1988.
[9] G.J. Kramer, Ph.D. dissertation, University of Amsterdam, 1990.
[10] L. Chinitz *et al.*, Phys. Rev. Lett. **67**, 568 (1991).
[11] Yanhe Jin, D.S. Onley, and L.E. Wright, Phys. Rev. C **45**, 1311 (1992).
[12] Yanhe Jin, J.K. Zhang, D.S. Onley, and L.E. Wright, Phys. Rev. C **47**, 2024 (1993).
[13] C. Giusti and F. Pacati, Nucl. Phys. **A473**, 717 (1987).
[14] C. Giusti and F. Pacati, Nucl. Phys. **A485**, 461 (1988).
[15] S. Boffi, C. Giusti, and F.D. Pacati, Nucl. Phys. **A435**, 697 (1985).
[16] Yanhe Jin and D.S. Onley, this issue, Phys. Rev. C **50**, 377 (1994).
[17] T. DeForest, Jr., Nucl. Phys. **A392**, 232 (1983).
[18] S. Hama, B.C. Clark, E.D. Cooper, H.S. Sherif, and R.L. Mercer, Phys. Rev. C **41**, 2737 (1990).
[19] S. Hama, B.C. Clark, E.D. Cooper, H.S. Sherif, and R.L. Mercer, Phys. Rev. C **47**, 297 (1993).
[20] P. Schwandt, H.O. Meyer, W.W. Jacobs, A.D. Bacher, S.E. Vigdor, M.D. Kaichuck, and T.R. Donoghue, Phys. Rev. C **26**, 55 (1982).